

# Interrogation of Global Active Site Occupancy of a Fungal Iterative Polyketide Synthase Reveals Strategies for Maintaining Biosynthetic Fidelity

Anna L. Vagstad,<sup>†</sup> Stefanie B. Bumpus,<sup>‡</sup> Katherine Belecki,<sup>†</sup> Neil L. Kelleher,<sup>§</sup> and Craig A. Townsend<sup>\*,†</sup>

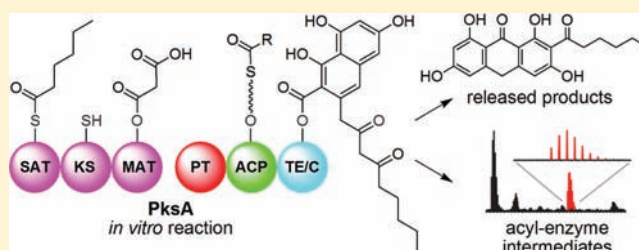
<sup>†</sup>Department of Chemistry, The Johns Hopkins University, Baltimore, Maryland, United States

<sup>‡</sup>The Institute for Genomic Biology, University of Illinois at Urbana–Champaign, Urbana, Illinois, United States

<sup>§</sup>Departments of Chemistry and Molecular Biosciences, Northwestern University, Evanston, Illinois, United States

## Supporting Information

**ABSTRACT:** Nonreducing iterative polyketide synthases (NR-PKSs) are responsible for assembling the core of fungal aromatic natural products with diverse biological properties. Despite recent advances in the field, many mechanistic details of polyketide assembly by these megasynthases remain unknown. To expand our understanding of substrate loading, polyketide elongation, cyclization, and product release, active site occupancy and product output were explored by Fourier transform mass spectrometry using the norsolorinic acid anthrone-producing polyketide synthase, PksA, from the aflatoxin biosynthetic pathway in *Aspergillus parasiticus*. Here we report the simultaneous observation of covalent intermediates from all catalytic domains of PksA from *in vitro* reconstitution reactions. The data provide snapshots of iterative catalysis and reveal an underappreciated editing function for the C-terminal thioesterase domain beyond its recently established synthetic role in Claisen/Dieckmann cyclization and product release. The specificity of thioesterase catalyzed hydrolysis was explored using biosynthetically relevant protein-bound and small molecule acyl substrates and demonstrated activity against hexanoyl and acetyl, but not malonyl. Processivity of polyketide extension was supported by the inability of a nonhydrolyzable malonyl analog to trap products of intermediate chain lengths and by the detection of only fully extended species observed covalently bound to, and as the predominant products released by, PksA. High occupancy of the malonyl transacylase domain and fast relative rate of malonyl transfer compared to starter unit transfer indicate that rapid loading of extension units onto the carrier domain facilitates efficient chain extension in a manner kinetically favorable to ultimate product formation.



## INTRODUCTION

Mass spectrometry is a powerful tool for studying the biosynthesis of secondary metabolites.<sup>1,2</sup> Spurred by technical advances in electrospray ionization Fourier transform mass spectrometry (ESI-FTMS), analysis of enzyme-bound intermediates is becoming an established biochemical tool to investigate the assembly of polyketide and nonribosomal peptide natural products. In these systems, biosynthetic intermediates are covalently sequestered on the enzyme during synthesis, necessitating techniques to resolve regiospecific mass shifts of active site peptides released through proteolysis. Intermediates are tethered as thioesters to a 4'-phosphopantetheine (Ppant) moiety installed post-translationally onto a carrier domain at a conserved serine. In addition to direct detection of active site peptides, the Ppant arm of the carrier protein, and anything covalently loaded on it as a terminal thioester, can be expelled for detection as a small molecule for high resolution mass spectrometric (MS) analysis.<sup>3</sup>

To date, MS strategies to visualize covalent intermediates have mainly been exploited for analysis of modular polyketide synthases (PKSs) and nonribosomal peptide synthetases

(NRPSs) composed of large multidomain modules each responsible for condensation of one extension unit in a collinear fashion.<sup>1,2</sup> On the other hand, iterative PKSs, such as the discrete bacterial enzymes and fungal multidomain systems, use substrate loading and condensation domains in successive catalytic cycles to achieve full-length products. Although iterative and modular PKSs share the same fundamental chain elongation step—the sequential condensation of malonyl derivatives—they have different demands for the coordination of oligoketide assembly. Iterative use of active sites requires that substrate specificity be flexible over the range of intermediate chain lengths. Additionally, substrate priming must be tightly controlled so that active sites do not become blocked nonproductively and unavailable for elongation pathways. In contrast, modular catalytic domains bind and react single stereochemically defined intermediates.

The fungal multidomain PKSs are phylogenetically related to mammalian fatty acid synthases (FASs) involved in the primary

Received: February 18, 2012

Published: March 27, 2012

metabolic synthesis of palmitate.<sup>4</sup> FASs contain the full complement of tailoring domains and following each extension, while tethered to the carrier protein, the  $\beta$ -keto position of the newly extended chain is completely reduced. The  $\beta$ -keto reductase (KR), dehydratase (DH), and enoyl reductase (ER) domains are responsible for the stepwise conversion from the ketone to the alcohol, alkene, and alkane, respectively. Alternatively, PKSs can vary the extent of processing at the  $\beta$ -carbon to achieve structural diversity. Reducing fungal PKSs program  $\beta$ -carbon functionality during chain extension through selective use of tailoring domains, whereas nonreducing systems lack reductive domains entirely and instead synthesize an unaltered poly- $\beta$ -keto carrier protein-bound intermediate.<sup>5</sup>

Prominent among the experimental challenges presented by iterative, multidomain enzymes are difficulties in heterologous expression and limitations in characterizing individual steps during catalysis. To overcome these barriers, we have focused on a “deconstruction” approach in which these megasynthase proteins are expressed as their constitutive domain fragments, typically as hexahistidine fusions in *Escherichia coli*, for selected recombination and *in vitro* analysis. Guided by *in silico* prediction of domain boundaries using the UMA algorithm, we previously reported the reconstitution of PksA from the filamentous fungus *Aspergillus parasiticus* responsible for assembling the polyketide precursor core of the potent carcinogenic mycotoxin, aflatoxin B1 (**1**).<sup>6,7</sup> The domain architecture of PksA follows the canonical pattern for nonreducing iterative polyketide synthase (NR-PKS) enzymes. From N- to C-terminus the domains include starter unit: acyl-carrier protein transacylase (SAT),  $\beta$ -ketoacyl synthase (KS), malonyl-CoA: acyl-carrier protein transacylase (MAT), product template (PT), acyl-carrier protein (ACP), and thioesterase/Claisen cyclase (TE/CLC). The substrate loading and condensation domains work in concert to assemble an ACP-bound linear polyketide. In the case of PksA, an octaketide intermediate is formed from a hexanoyl starter unit combined with seven malonyl extension units; however, enzymes from the NR-PKS family synthesize a wide assortment of natural products that incorporate a number of different starter units and chain lengths.<sup>8</sup>

The domain architecture and expected enzyme-bound intermediates of PksA are summarized in Figure 1. In the native host, hexanoyl is synthesized by a dedicated yeast-like FAS and is introduced onto the PksA ACP by the SAT domain; *in vitro*, however, hexanoyl-CoA can substitute as acyl donor.<sup>9</sup> Transacylation of the starter unit to the KS domain and loading of malonyl onto the ACP by the MAT domain primes the enzyme for the first round of decarboxylative thio-Claisen condensation catalyzed by the KS. Following extension, the growing polyketide (now two carbons longer than the previous intermediate) is returned to the KS, and ACP is primed with another unit of malonate. Iterative condensation ensues, requiring that the KS bind and catalyze chain extension for enzyme-bound substrates ranging from 6 to 18 carbons in length. The final iteration results in an ACP-bound linear octa- $\beta$ -keto of 20 carbons.

Previous characterization of *in vitro* reaction products demonstrated the essential roles of the PT and TE domains for cyclization and product release to the first isolable intermediate in aflatoxin biosynthesis, norsolorinic acid anthrone (noranthrone, **2**), as shown in Figure 2.<sup>7</sup> Reactions lacking TE produced a new metabolite. This alternative product was identified as the isomeric species norsolorinic acid pyrone

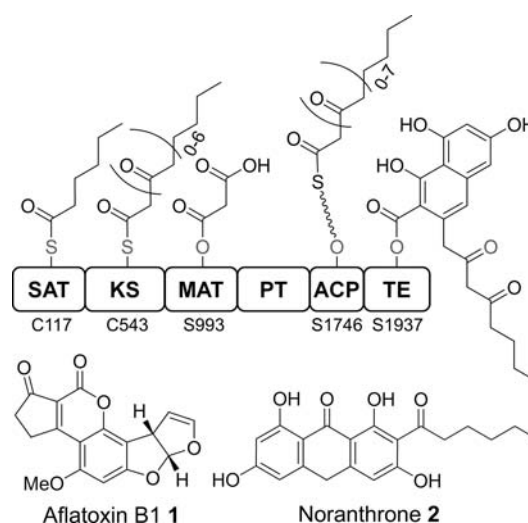


**Figure 1.** PksA domain architecture and expected on-pathway enzyme-bound species. Noranthrone is the first isolable intermediate in the aflatoxin biosynthetic pathway.

(norpyrone, **4**), which retains the regio-specific cyclizations of the A and B rings. Without the TE, the enolized ketone oxygen at C13 of bicyclic intermediate **7** can spontaneously close on the ACP-thioester resulting in an  $\alpha$ -pyrone C-ring. The TE domain catalyzes transesterification of **7** to a conserved serine and Claisen/Dieckmann-type third-ring cyclization to afford **2**. *In vitro*, autooxidation produces norsolorinic acid (**3**); however, *in vivo*, this conversion is catalyzed by a pathway specific monooxygenase, HypC.<sup>10</sup> Furthermore, reactions lacking the PT domain lost the ability to catalyze the C4–C9 and C2–C11 cyclization events required for the production of the norsolorinic scaffold. The recent biochemical and structural characterizations of the PT and TE cyclization domains give mechanistic insights into the conversion of the highly reactive linear polyketide intermediate **5** into the tricyclic product.<sup>11,12</sup> Other classes of PTs have been characterized and catalyze first-ring cyclizations of C2–C7, as in bikaverin biosynthesis in *Gibberella fujikuroi* by Pks4,<sup>13</sup> or C6–C11, as in asperthecin biosynthesis in *Aspergillus nidulans* by AptA.<sup>14</sup>

Covalent adducts of the PksA ACP were also identified, corroborating results from *in vitro* product analysis.<sup>7</sup> ACP-bound intermediates from reactions lacking the TE domain were considered. Reactions with or without the PT domain yielded remarkably similar MS profiles. Only hexanoyl and malonyl substrates, acetyl (resulting from the nonproductive decarboxylation of malonyl), and full-length intermediates were observed. The substrate loading and condensation domains (SAT-KS-MAT) in conjunction with just the ACP were sufficient to synthesize the C<sub>20</sub>-linear intermediate **5**, confirming that chain length is minimally controlled by the KS domain.

To further our understanding of polyketide assembly, we wished to observe the active site occupancies of all PksA domains in parallel. Here we report the simultaneous detection of acyl intermediates at the catalytic residues of up to five domains (SAT-C117, KS-C543, MAT-S993, ACP-S1746, and TE-S1937) in a series of *in vitro* experiments. PT catalyzes cyclization noncovalently<sup>11</sup> and could not be monitored using these MS techniques. In addition to acyl-enzyme analysis, products released from the enzyme were also characterized to explore the biosynthetic potential of PksA. Taken together,

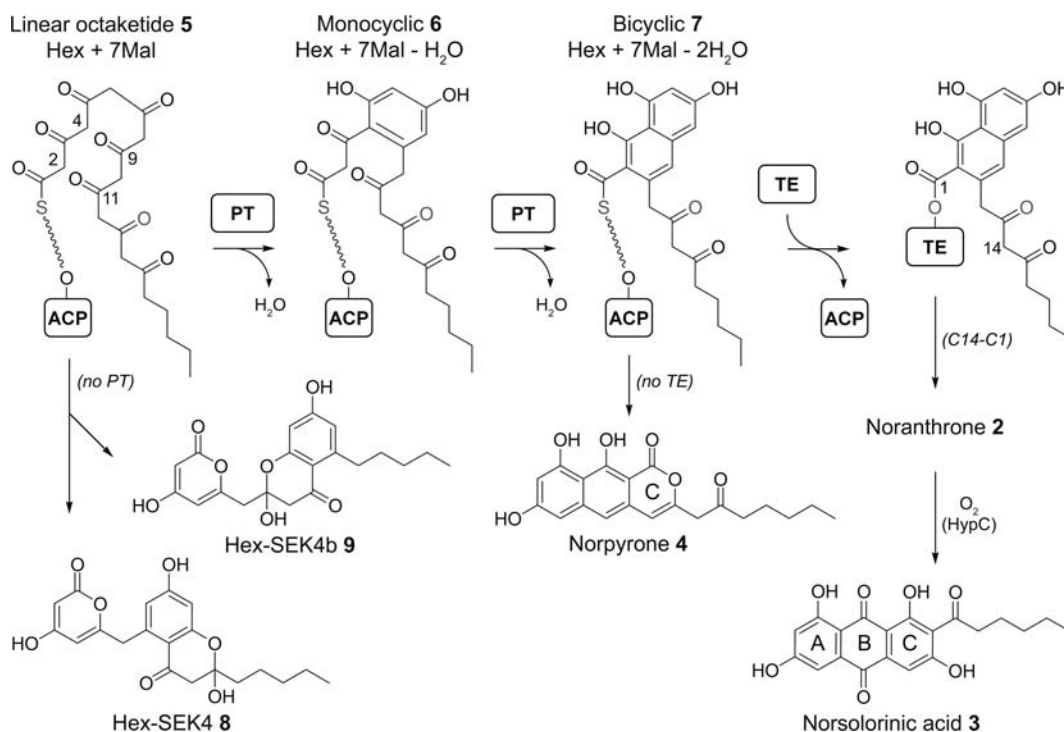


**Figure 2.** Extended ACP-bound intermediates and major *in vitro* products of PksA reactions.

these data support the view that polyketide extension is highly processive and that the TE domain has an editing function in addition to its biosynthetic role.

## EXPERIMENTAL SECTION

**Reagents.** All chemicals were purchased from Sigma Aldrich (St. Louis, MO) unless otherwise noted. [1-<sup>14</sup>C]-hexanoyl-CoA, [1-<sup>14</sup>C]-acetyl-CoA, and [2-<sup>14</sup>C]-malonyl-CoA were purchased from American Radiolabeled Chemicals (St. Louis, MO), NEN Radiochemicals (Waltham, MA), and Morovek (Brea, CA), respectively. Ni-NTA resin was from Qiagen (Valencia, CA).

**Cloning.** Cloning details for all constructs are provided in the Supporting Information. Expression plasmids used in this study are summarized in Table S1. Primers are given in Table S2. Mutations were generated by overlap extension PCR. DNA manipulations were carried out in *E. coli* DH5 $\alpha$  or BL21(DE3) using standard methods<sup>15</sup> and expression constructs were confirmed by automated sequencing (Johns Hopkins University Synthesis and Sequencing Facility, Baltimore, MD).

**Protein Expression and Purification.** PksA domains were heterologously expressed and purified and ACP-containing proteins optionally pantetheinylated as previously described.<sup>7</sup> Following purification, proteins could be frozen in storage buffer [100 mM K/PO<sub>4</sub> pH 7.5, 10% glycerol, 2 mM dithiothreitol (DTT)] or used immediately. Proteins were dialyzed against assay-specific buffer prior to *in vitro* analysis. Protein concentrations were determined by Bradford assay in at least duplicate using bovine albumin as the standard and protein dye-reagent (Bio-Rad, Hercules, CA).

**Reverse Phase Liquid Chromatography (RPLC)-Fourier Transform Mass Spectrometry (FTMS) Analysis.** For the enzyme-bound intermediate data presented in this study, all proteins were used at 10  $\mu$ M concentration in 100 mM K/PO<sub>4</sub> pH 7.4. When required, hexanoyl-CoA substrate was provided at 0.5 mM and malonyl-CoA was provided at 2 mM concentrations. The 50  $\mu$ L reactions were initiated by substrate addition and stopped by flash freezing in liquid nitrogen after 60 min at room temp. Samples were shipped on dry ice and stored at -80  $^{\circ}$ C prior to RPLC-FTMS analysis.

Reactions were thawed at room temp before enzymatic digestion. An aliquot of each reaction was removed and incubated in 100  $\mu$ M NH<sub>4</sub>HCO<sub>3</sub> (pH 8) with 2 mM tris(2-carboxyethyl) phosphine (TCEP) (pH 6) at room temp for 5 min. Sequencing-grade trypsin (Promega, Madison, WI) was added in a ratio of 1:5 w:w trypsin:total protein and incubated at 30  $^{\circ}$ C for 20 min. Prior to addition, the trypsin was dissolved in Promega trypsin resuspension buffer and activated at 30  $^{\circ}$ C for 15 min; 20  $\mu$ L of resuspension buffer was used per 20  $\mu$ g of trypsin. Digestion reactions were quenched by addition of an equal reaction volume of 10% formic acid and frozen at -80  $^{\circ}$ C.

All RPLC analyses were conducted using a Jupiter C4 column (1.0  $\times$  150 mm, 5  $\mu$ , Phenomenex, Torrance, CA). All FTMS analyses were conducted using an LTQ-FT hybrid ion trap-FTMS (Thermo Fisher Scientific, Waltham, MA) operating at 11 T. Digested samples were injected directly onto the RPLC column and eluted into the mass spectrometer using a linear gradient starting at 95% solvent A/5% solvent B and ramping to 5% solvent A/95% solvent B over 1 h, where solvent A was water +0.1% formic acid and solvent B was acetonitrile +0.1% formic acid. All FTMS analysis methods included a full scan (detect  $m/z$  400–2000), source induced dissociation (SID) for the Ppant ejection assay<sup>3</sup> (SID = 75 V, detect  $m/z$  250–600), and data dependent tandem MS (MS/MS) using collision induced dissociation (CID) with FT detection on the top three peptide species in each full scan. MS/MS data were analyzed using ProSightPC v2.0 (Thermo Fisher Scientific). All other data were analyzed using the Qualbrowser software suite provided with the LTQ-FT instrumentation (Thermo Fisher Scientific). Theoretical and experimental masses of all peptides discussed are provided in Table S3. Theoretical structures and masses of Ppant ejection ions are shown in Figure S1.

**HPLC Analysis of Released Enzymatic Products.** *In vitro* reactions were executed as previously described with some alterations.<sup>7</sup> Briefly, reactions containing 10  $\mu$ M each protein in 100 mM K/PO<sub>4</sub> pH 7.0 were initiated by addition of acyl-CoA substrates. After 12 h, 500  $\mu$ L reactions were quenched with 10  $\mu$ L 6N HCl and extracted three times with 1 mL ethyl acetate. Pooled extracts were dried with anhydrous Na<sub>2</sub>SO<sub>4</sub> and evaporated to dryness using a Speedvac. Products were dissolved in 500  $\mu$ L 40% aqueous acetonitrile and chromatographed (100  $\mu$ L injections) over a Prodigy ODS3 analytical column (4.6  $\times$  250 mm, 5  $\mu$ , Phenomenex) by a gradient HPLC method to resolve early eluting peaks using an Agilent 1200 (Santa



Clara, CA) instrument equipped with an autosampler. Bisolvent method: hold 40% B 10 min, linear gradient 40 to 85% B over 15 min, hold 85% B 10 min, and re-equilibrate to 40% B with a flow rate of 1 mL/min. SAT-KS-MAT (R1018A and wild-type) + PT-ACP reactions were further tested with 0.1, 0.5, or 1 M guanidinium to see if MAT activity could be restored through chemical complementation. The pH of the guanidine-HCl stock solution was adjusted to neutral using NaOH prior to addition. Selected reactions were additionally analyzed by HR-ESI-LCMS on a Shimadzu LC-IT-TOF over a Luna C18(2) analytical column (2.0 × 150 mm, 3 μm, Phenomenex) using a gradient of 20 to 80% B over 30 min with a flow rate of 0.2 mL/min.

**MS and NMR Characterization of Spontaneous Cyclization Products 8 and 9.** Small scale PT-less *in vitro* reactions were optimized for production of 8 and 9 with respect to domain concentration using acyl-CoA substrates (Table S5). Scaled-up reactions for isolation of the products used synthetic hexanoyl-SNAC starter unit and *in situ* generation of malonyl-SNAC extension units by the MatB system.<sup>16</sup> The malonyl CoA synthetase gene was cloned from *Rhizobium leguminosarum* gDNA and inserted into pET-28b at NdeI and HindIII sites to generate the N-terminal His<sub>6</sub>-tagged construct. MatB was heterologously expressed from Luria–Bertani broth cultures of BL21(DE3) transformed with the pEMatB plasmid overnight at room temp induced with 1 mM IPTG. Enzyme was purified by Ni<sup>2+</sup> affinity chromatography and dialyzed against storage buffer, concentrated to ~20 mg/mL, flash frozen, and stored at -80 °C until use. Final reaction conditions were 5 μM SAT-KS-MAT, 40 μM *holo*-ACP, 5 μM TE, 2.5 mM hexanoyl-SNAC, 30 mM sodium malonate, 5 mM N-acetyl cysteamine (SNAC), 10 mM MgCl<sub>2</sub>, 7 mM ATP, 0.56 mg/mL MatB, 100 mM K/PO<sub>4</sub> pH 7.5, 10% glycerol, and 1 mM TCEP. The reaction mixture was filtered through a 0.2 μm Steriflip filtration device (Millipore, Billerica, MA) to prevent bacterial growth during extended incubation. After approximately 48 h, reactions were acidified to precipitate protein and the products extracted into ethyl acetate. Solvent was evaporated, products dissolved in 30% aqueous acetonitrile, and baseline resolution of the closely related products was ultimately accomplished using a 29% Solvent B isocratic method over a Prodigy ODS3 analytical column (4.6 × 250 mm, 5 μm, Phenomenex) with a flow rate of 1.25 mL/min (Figure S11). HPLC purified product was collected and lyophilized from several 30 mL reactions.

Purified 8 and 9 were subjected to high resolution mass fragmentation on a Shimadzu IT-TOF (Figures S12 and S16). NMR characterization was determined at 25 °C in d<sub>6</sub>-DMSO by 1D-<sup>1</sup>H and 2D-long-range <sup>1</sup>H-<sup>13</sup>C gHSQC experiments on ~3 mg samples of compound. Spectra were acquired on a 500 MHz (<sup>1</sup>H) Varian INOVA spectrometer equipped with a triple-resonance z-gradient probe. Further details are provided in the Supporting Information. Data were processed using SpinWorks 3.0 or ACD/NMR Processor v12.01 software.

**Spectrophotometric Acyl-SNAC TE Hydrolysis Assay.** TE-catalyzed hydrolysis of acyl-SNAC substrates was followed by a continuous spectrophotometric assay using a Cary 50 instrument (Varian Inc., Walnut Creek, CA).<sup>17</sup> The free thiol of SNAC reacted with Ellman's reagent [5,5'-dithio-bis(2-nitrobenzoic acid), DTNB] to release the yellow-colored 2-nitro-5-thiobenzoate dianion detected at 412 nm. Background rate was corrected for by comparison to an S1937A inactive mutant. Each 100 μL reaction contained variable concentrations of substrate, 200 μM DTNB, and 2 μM TE in 100 mM K/PO<sub>4</sub> pH 7.0. Acetyl-SNAC was tested at 2.5–75 mM and hexanoyl-SNAC was tested at 0.5–7.5 mM ranges. Reactions were initiated by addition of TE and initial rates were calculated for the first 30 s of reaction using a molar absorptivity of 14150 M<sup>-1</sup>cm<sup>-1</sup>.<sup>18</sup> Kinetic constants were determined by fitting initial velocity data at various substrate concentrations to Michaelis–Menten parameters using nonlinear regression with KaleidaGraph v4 (Synergy Software, Reading, PA). Acyl-SNAC thioesters were synthesized as previously described.<sup>19</sup>

**Radiochemical Acyl-enzyme TE Hydrolysis Assays.** Individual reaction conditions for TE hydrolysis assays are summarized below for each protein set. Acyl-ACP was generated by activation with <sup>14</sup>C-labeled hexanoyl-, acetyl-, or malonyl-CoA using the phosphopante-

thetyl transferase Svp.<sup>20</sup> SAT, KS, and MAT were loaded by preincubation with labeled CoAs. Reactions were carried out at room temp, quenched with loading dye, separated by SDS-PAGE, dried between cellophane sheets or on filter paper using a gel dryer (Hoeffer Scientific, Holliston, MA), and visualized by autoradiography (Kodak Biomax XAR film) or phosphorimaging (Typhoon 9410 Imager, GE Healthcare, Uppsala Sweden, Johns Hopkins University Integrated Imaging Center). Reactions with either no TE or the S1937A variant were used as negative controls. DTT and 2-mercaptoethanol reducing agents were excluded from the loading dye since they are known to cleave acyl-ACP species.<sup>21</sup> TCEP was included in the reactions to maintain reducing conditions.

For the didomain acyl-ACP substrate assay, reactions contained 15 μM ACP-TE, 75 μM <sup>14</sup>C-labeled acyl-CoA, 1.5 μM Svp, 10 mM MgCl<sub>2</sub>, 50 mM Tris pH 7.5, 5% glycerol; 20 μL aliquots were quenched at 45 min.

For the monodomain acyl-ACP assay, 100 μM ACP was treated with 5 μM Svp, and 400 μM total acyl-CoA (mixture of unlabeled and <sup>14</sup>C-labeled to achieve 10 μCi/mL) in 100 mM K/PO<sub>4</sub> pH 7.0, 10 mM MgCl<sub>2</sub>, 1 mM TCEP, and 10% glycerol for 45 min at room temp. TE was prealiquoted and reactions initiated by addition of acyl-ACP. Final conditions were 10 μM acyl-ACP with 0, 3, 1, 0.33, 0.11, 0.04, or 0.01 μM TE or 3 μM TE S1937A in 100 mM K/PO<sub>4</sub> pH 7.0 and 10% glycerol quenched at 6 min.

TE hydrolysis activity directly toward SAT, KS, and MAT was also measured. Since KS and MAT monodomains are not amenable to soluble expression, the N-terminal domains were examined in the context of the SAT-KS-MAT construct, where double active site mutations were generated to isolate the activity of a single domain. SAT-KS-MAT (12.5 μM) with active SAT or KS were preincubated with 125 μM [<sup>14</sup>C]-hexanoyl-CoA and MAT was incubated with 125 μM [<sup>14</sup>C]-malonyl-CoA for 10 min. Reactions were initiated by addition of either buffer (no TE), TE S1937A, or TE wild-type. Reactions (80 μL) contained 10 μM SAT-KS-MAT, 100 μM <sup>14</sup>C-acyl-CoA, 5 μM TE, 100 mM K/PO<sub>4</sub> pH 7.0, 10% glycerol, and 0.5 mM TCEP; 20 μL aliquots were quenched at 5, 15, and 30 min.

**Malonyl Carba(dethia) Coenzyme A.** The nonhydrolyzable analog, malonyl (carba)dethia coenzyme A (17), was synthesized similarly to that previously described.<sup>22</sup> The synthetic malonyl methyl ester dethia pantetheine intermediate was enzymatically converted to the CoA analog product in a one-pot *in vitro* reaction using pig liver esterase (PLE) and *E. coli* CoA biosynthetic enzymes.<sup>23</sup> The crude preparation of PLE (Sigma Aldrich) was found to have contaminating phosphatase activity toward the 3' position of the CoA analog and, therefore, the methyl ester was enzymatically deprotected as the pantetheine derivative prior to treatment with the CoA biosynthetic enzymes. Lyophilization of HPLC purified 17 resulted in ~20% decarboxylation. Further details are provided in the Supporting Information (Figures S20 and S21).

Covalent loading of the analog onto PksA ACP monodomain was confirmed by MALDI (Table S8) using α-cyano-4-hydroxy-cinnamic acid (CHCA) matrix and a Bruker AutoFlexIII instrument (Bruker Daltonics, Billerica, MA). The SAT-KS-MAT + ACP protein combination was selected as test subject. SAT-KS-MAT (20 μM) and *holo*-ACP (10 μM) were separately preincubated with either pentanoyl-SNAC, hexanoyl-SNAC, heptanoyl-SNAC, or hexanoyl-CoA starter units for 15 min to generate component A. ACP (50 μM) was separately activated with 200 μM analog to generate malonyl-C-ACP giving component B. For no-extension-unit control reactions, A and B were mixed in 2:1, 1:1, and 1:2 ratios for each starter unit as a positive control to determine what ratio of protein gave the best yield of the hex + analog diketide species (Figure S22 and Table S9). Component A was subsequently pretreated with 2 mM malonyl-CoA for one min and then combined with B in a 1:1 ratio. Following incubation overnight at room temp, all reactions were quenched in liquid nitrogen and stored at -80 °C pending analysis.

**HPLC Chromatographic Transacylase Assay.** The HPLC-based transacylase assay was conducted as previously described for SAT monodomains<sup>9,24</sup> substituting SAT-KS-MAT tridomain mutants. Briefly, reactions containing 1 mM acyl-CoA donor and 2.5 mM

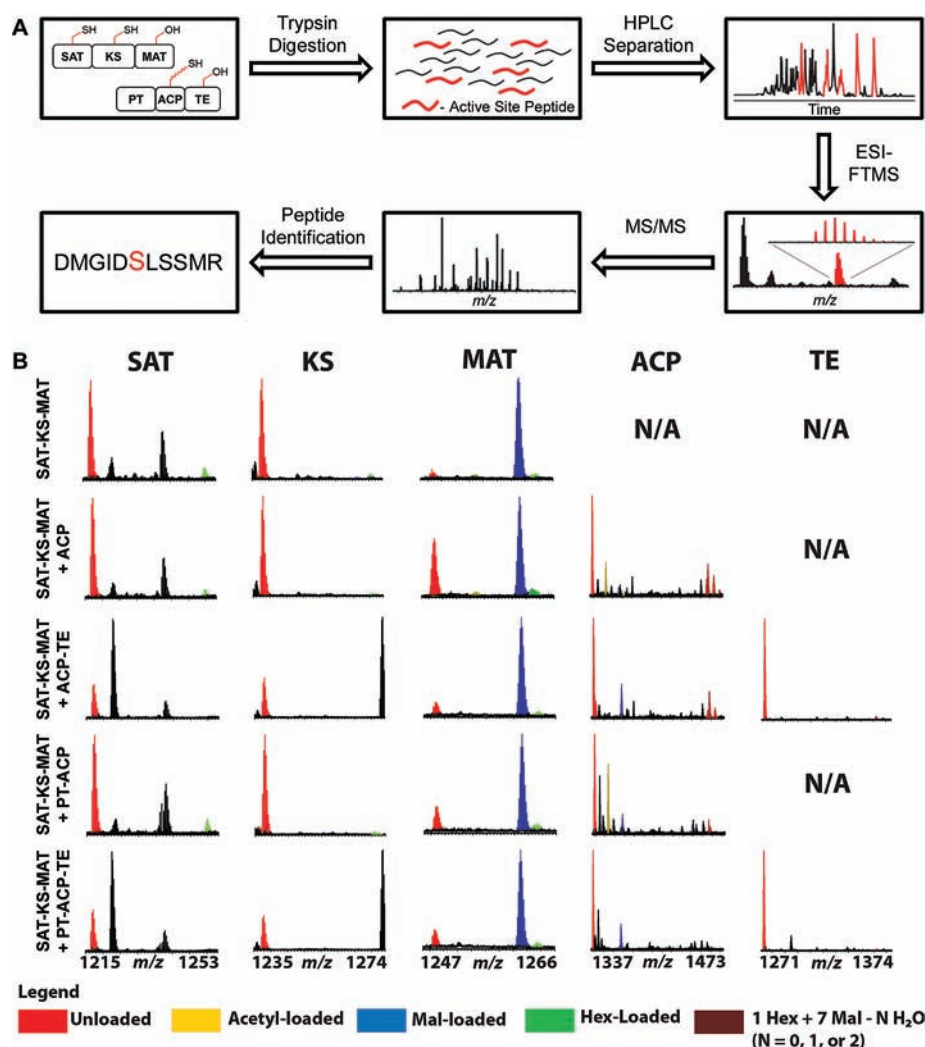


**Figure 3.** Analysis of enzyme-bound PksA intermediates. (A) Methods schematic. Selected proteins are combined *in vitro* with substrates. Following trypsin digest, peptides are separated by RP-HPLC in-line with ESI-FTMS to identify active site peptides and their acyl mass shifts. (B) Summary of observed domain occupancies of SAT, KS, MAT, ACP, and TE active site peptides for hexanoyl- and malonyl-CoA reactions. Identities of the bound acyl-species are color-coded.

panetheine acceptor were initiated by enzyme addition and incubated at 28 °C. Aliquots were withdrawn at 2, 4, 6, and 8 min time points and quenched with 8 M urea. Following separation over a Luna phenyl-hexyl analytical column (4.6 × 250 mm, 5 μ, Phenomenex), free CoA production was quantified using a standard curve to determine relative rates of transfer. Enzyme concentration was adjusted so that production remained linear during the assay.

**Radiochemical Transacylase Assay.** Transacylase activity of SAT, KS, and MAT domains toward hexanoyl and malonyl substrates onto ACP was tested by a radiochemical transacylase assay.<sup>9</sup> Individual domain activities were isolated by mutagenesis of multiple active sites in the context of the SAT-KS-MAT tridomain. The triple knockout (C117A-C543A-S993A) was used as a negative control for nonspecific protein effects. PT-ACP didomain was used as the acceptor. Reactions contained 15 μM of each protein incubated with 100 μM <sup>14</sup>C-labeled hexanoyl- or malonyl-CoA. Aliquots were quenched with 4× SDS-loading dye at 10 min and separated by 12% SDS-PAGE. Gels were dried between cellophane sheets and analyzed by autoradiography.

## RESULTS

**Simultaneous Detection of Active Site Peptides.** The effect of the cyclization and carrier domains on substrate loading and polyketide assembly was assessed *in vitro* by excluding the PT, ACP, and TE domains individually and in

groups (Figure 3). Protein combinations included: (1) SAT-KS-MAT, (2) SAT-KS-MAT + ACP, (3) SAT-KS-MAT + ACP-TE/CLC, (4) SAT-KS-MAT + PT-ACP, and (5) SAT-KS-MAT + PT-ACP-TE/CLC. Following reaction, proteins were cleaved with trypsin, and active site peptides were identified from the complex mixture by RPLC-FTMS and confirmed by MS/MS fragmentation (Figure 3A). Although proteolytic conditions optimized for minimal (thio)ester hydrolysis were used, it is possible that unequal rates of hydrolysis during workup may contribute to a bias in the observed acyl profiles. Changes in ionization efficiency due to acyl modification of active site peptides were assumed to be negligible.

To establish the degree of background substrate loading occurring *in vivo* during heterologous expression of proteins in *E. coli* that was maintained through the enzyme purification process, protein combinations with excluded exogenous acyl-CoA substrates were examined for evidence of covalent adducts. SAT, KS, ACP, and TE active sites were completely vacant and the MAT domain only retained trace levels of acetyl and malonyl, providing a clean baseline for profiling acyl-enzyme species.

All protein combinations were tested with hexanoyl and malonyl substrates. A summary of active site occupancy profiles for these reactions is provided in Figure 3B and a comprehensive analysis of species is available as tables and figures in the Supporting Information. The relevant mass range for each active site peptide and its various acylation states is shown and peaks are color coded by the identity of the acyl species. Peaks in black correspond to other peptides that happen to fall into these mass ranges and can differ by protein combination depending on which domains are present in the reaction. SAT and MAT transferase domains bound their respective hexanoyl and malonyl substrates (Figure 3B, top row). Despite extensive efforts to visualize intermediate chain lengths, under all experimental parameters tested only monomeric substrates or full-length octaketides were observed. No extended polyketides were detected on the KS, only hexanoyl starter units, indicating that extension is rapid and processive. In accord with previous results,<sup>7</sup> octaketide species corresponding to masses for linear, singly dehydrated, and doubly dehydrated poly- $\beta$ -keto intermediates were observed. In addition, hexanoyl and malonyl substrates and the non-productive decarboxylation product, acetyl, were found on the ACP. Reactions with and without the PT showed little variation in the profile of acyl-adduct masses across all domains. One exception was that the distribution of ACP-bound octaketide intermediates shifted toward the doubly dehydrated species with inclusion of PT, consistent with its activity as a two-ring cyclase. Acyl-ACP species were confirmed by their Ppant ejection ions (Figure S1). Previous analysis of the MS/MS data for the bicyclic-ACP ion and the UV signature were consistent with a correctly cyclized C4–C9/C2–C11 species.<sup>7</sup> Structural analyses of the ACP-bound octaketides were not considered for this study. A single mass peak may represent multiple isomeric species with the same extent of dehydration resulting from either PT-catalyzed or spontaneous cyclization events. Likewise, the TE accumulated low levels of a doubly dehydrated intermediate that is probably the on-pathway C4–C9/C2–C11 bicyclic product of the PT; however, we could not strictly exclude the possibility that other species were represented.

The most conspicuous observation from these experiments was the decrease in amount and variety of covalent species across multiple domains when TE/CLC was present. This result led to the hypothesis that the TE plays a marked editing role—apart from its normal synthetic function as a Claisen/Dieckmann cyclase—by removing stalled acyl adducts from the enzyme to facilitate efficient overall biosynthesis. The inclusion of TE afforded occupancy profiles with no detectable acetyl-MAT or acetyl-ACP. Hexanoyl species were also notably absent from the SAT, KS, and ACP domains. In contrast, the MAT domain remained heavily acylated with malonyl whether or not TE was present.

To examine how acyl loading was affected by withholding substrates, all protein combinations were further tested with either hexanoyl-CoA starter units or malonyl-CoA extension units separately for comparison to the bisubstrate reactions. The ACP occupancy for the SAT-KS-MAT + ACP reactions, depicted in Figure 4, was selected as a representative example. Detailed species analyses are given in Figure S7. When malonyl alone was provided to the SAT-KS-MAT + ACP combination, nearly stoichiometric levels of malonyl were found on the ACP (Figure 4B). Acetyl-ACP was barely detectable, demonstrating that KS has no appreciable decarboxylase activity toward

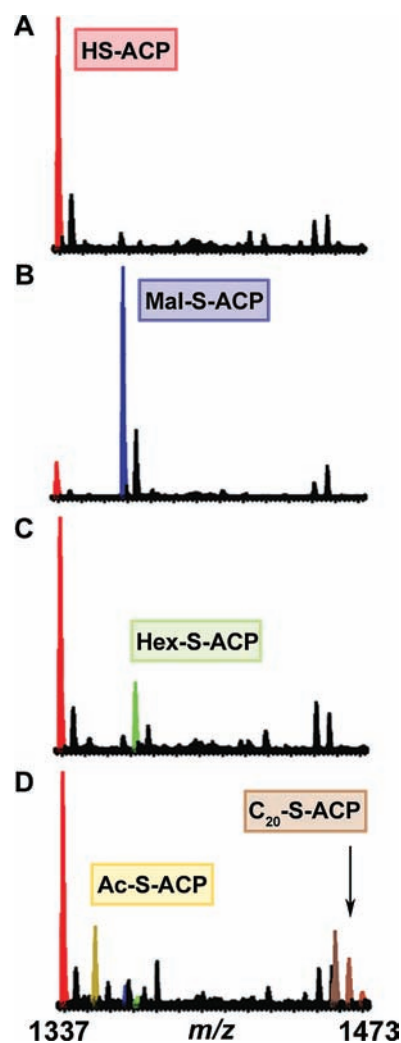


**Figure 4.** PksA-ACP active site occupancy profiles for the SAT-KS-MAT + ACP combination with either (A) no substrates, (B) malonyl-CoA only, (C) hexanoyl-CoA only, or (D) hexanoyl- and malonyl-CoA substrates.

malonyl-ACP in the absence of the correct starter unit or properly extending polyketide chain. In contrast to high malonyl occupancy, starter unit loading was modest when hexanoyl was provided alone (Figure 4C) or in tandem with malonyl (Figure 4D). Comparison of two-substrate to malonyl-only reactions showed decreased extent of acylation of the ACP from nearly stoichiometric malonylation to low occupancy with a mixture of substrates and octaketide species evident. Starter unit loading appears to promote ACP vacancy, preventing congestion with extension units and freeing the enzyme for polyketide extension.

In general, observed species were in line with domain function, though some unexpected adducts were observed. These aberrant species included low levels of hexanoyl on the MAT domain, which were more apparent in enzymes incubated with hexanoyl alone. The wild-type MAT domain of animal FAS is known to exhibit some medium chain-length transacylase activity, so this buildup of atypical intermediates is not necessarily surprising.<sup>25</sup> The SAT-KS-MAT reaction showed nominal levels of anomalous malonyl and acetyl on the KS domain. These species were attributed to nonspecific transacylation from CoA thioesters that occurred in the absence of

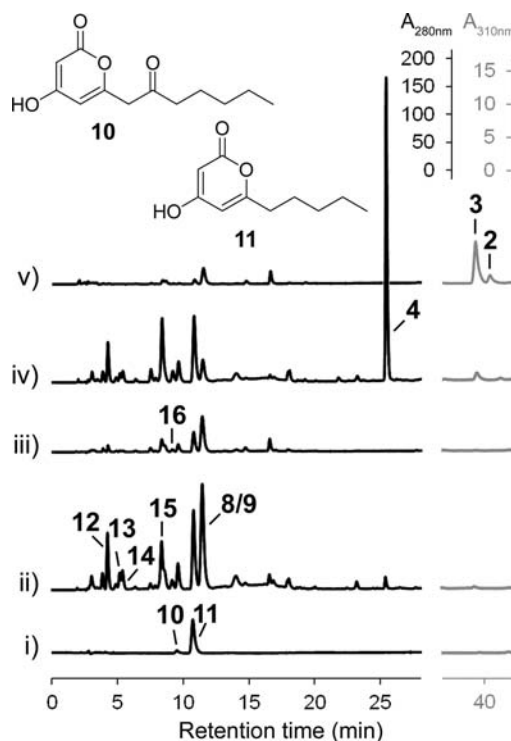


the carrier domain and are not considered physiologically relevant.

**Characterization of Released *in vitro* Reaction Products.** *In vitro* PksA reaction products were previously analyzed by an isocratic HPLC method with comparison to authentic standards to identify norsolorinic acid (**3**) as the autoxidized product of a complete set of domains and norpyrone (**4**) as the default product of TE-less reactions.<sup>7</sup> It was noted that other species were present in the solvent front of HPLC chromatograms. To more fully explore the biosynthetic potential of PksA, a gradient method was developed to resolve early eluting products from enzymatic reaction extracts. The SAT-KS-MAT construct was combined with all relevant permutations of intact and dissected PT, ACP, and TE domain fragments. Molecular weight data were collected by high resolution LC-ESI-MS in the positive ion mode for selected reactions. Confinement to chemical variations permitted under the rules governing nonreductive polyketide assembly allowed the chain length, number of dehydrations, and manner of product release, along with any postsynthetic transformations (such as spontaneous decarboxylation or oxidation events) to be assigned for each mass detected. Diode array UV-vis spectra extracted from HPLC chromatograms provided further insight into structure and regioselectivity of polyketide cyclization for each product. Comprehensive analyses of the observed products are provided in Figure S8 with a selected set of reactions presented in Figure 5.

Hexanoyl-primed tetraketide (Hex + 3 Mal, **10**) and triketide (Hex + 2 Mal, **11**) pyrones are evident in SAT-KS-MAT only reactions indicating that, to a limited extent, KS can directly utilize hexanoyl- and malonyl-CoAs as substrates in place of the ACP-shuttled building blocks, resulting in short chain-length poly- $\beta$ -keto-CoA intermediates. The diketide-CoA is expected to be reasonably stable and able to transacylate back to the KS for further extension. The triketide-CoA can either transesterify back to KS or terminate extension by undergoing spontaneous cyclization to pyrone **11**. The tetraketide intermediate is evidently sufficiently labile (prone to enolization) that pyrone formation outcompetes further extension, thus capping chain length for SAT-KS-MAT only reactions at the C<sub>12</sub>-pyrone product **10**. Comparable reactions where each domain in the SAT-KS-MAT construct was independently inactivated by mutagenesis of the active site nucleophile to alanine were also investigated (Figure S10). The KS-blocked mutant lost the ability to generate **10** and **11**, confirming that their production is KS-dependent. Likewise, if malonyl-SNAC was used, neither product was detected, indicating that the phosphopantetheine moiety is essential for the ACP-less delivery of extension units to the KS. Consistent with this view, synthesis was independent of the MAT domain since malonyl-CoA was used directly. Inactivation of the SAT domain had the interesting effect of increasing yields of the pyrones. When SAT acylation was prevented through mutagenesis, KS activity (as measured by output of **10** and **11**) increased approximately 5-fold. These short chain-length pyrones are analogous to the triacetic lactone derailment product commonly observed as a shunt metabolite in fatty acid biosynthesis, particularly in the absence of reductant (NADPH).<sup>26</sup>

Addition of ACP enabled biosynthesis of full-length products. As previously observed,<sup>7</sup> PT promoted C4–C9 and C2–C11 cyclizations and aromatizations to generate the ACP-bound bicyclic intermediate **7**, which was either released



Prod.	RT (min)	Mol. Formula	Chain Length	Dehyd.	Release, Other
<b>12</b>	4.2	C <sub>16</sub> H <sub>20</sub> O <sub>6</sub>	Hex+5Mal	-H <sub>2</sub> O	+H <sub>2</sub> O
<b>13</b>	5.1	C <sub>18</sub> H <sub>22</sub> O <sub>7</sub>	Hex+6Mal	-H <sub>2</sub> O	+H <sub>2</sub> O
<b>14</b>	5.4	C <sub>18</sub> H <sub>22</sub> O <sub>7</sub>	Hex+6Mal	-H <sub>2</sub> O	+H <sub>2</sub> O
<b>15</b>	8.3	C <sub>18</sub> H <sub>20</sub> O <sub>6</sub>	Hex+6Mal	-2H <sub>2</sub> O	+H <sub>2</sub> O
<b>16</b>	9.1	C <sub>18</sub> H <sub>20</sub> O <sub>6</sub>	Hex+6Mal	-2H <sub>2</sub> O	+H <sub>2</sub> O
<b>10</b>	9.5	C <sub>12</sub> H <sub>16</sub> O <sub>4</sub>	Hex+3Mal	–	O-C
<b>11</b>	10.7	C <sub>10</sub> H <sub>14</sub> O <sub>3</sub>	Hex+2Mal	–	O-C
<b>8/9</b>	11.4	C <sub>20</sub> H <sub>22</sub> O <sub>7</sub>	Hex+7Mal	-H <sub>2</sub> O	O-C
<b>4</b>	25.2	C <sub>20</sub> H <sub>20</sub> O <sub>6</sub>	Hex+7Mal	-2H <sub>2</sub> O	O-C
<b>3</b>	39.3	C <sub>20</sub> H <sub>18</sub> O <sub>7</sub>	Hex+7Mal	-2H <sub>2</sub> O	C-C,[O]
<b>2</b>	40.5	C <sub>20</sub> H <sub>20</sub> O <sub>6</sub>	Hex+7Mal	-2H <sub>2</sub> O	C-C

**Figure 5.** HPLC analysis of *in vitro* PksA products for variable domain combinations. (i) SAT-KS-MAT + ACP, (iii) SAT-KS-MAT + ACP-TE/CLC, (iv) SAT-KS-MAT + PT-ACP, and (v) SAT-KS-MAT + PT-ACP-TE/CLC. The complete domain set produces noranthrone (**2**) which spontaneously oxidizes to norsolorinic acid (**3**). Reactions lacking the C-terminal TE domain produce norpyrone (**4**). Reactions lacking PT make a mixture of hex-SEK4 (**8**) and hex-SEK4b (**9**) as the major products. Hexanoyl primed tetraketide (**10**) and triketide (**11**) pyrones are also evident, as well as several truncated hydrolysis products, **12**–**16**. MS analysis of product peaks enabled the chain length and cyclization mode to be established. Retention time, molecular formula, number of dehydrating cyclizations, mode of product release, and postsynthetic oxidation are reported in the table.

spontaneously as the pyrone **4** or by TE catalyzed transesterification and Claisen cyclization to the anthrone **2**, depending on included domains. Norsolorinic acid (**3**) spontaneously forms from **2** when exposed to air. Although care was taken to treat each reaction equally, during work-up and HPLC analysis samples are inevitably exposed to air for varying amounts of time, hence the ratio of **2** to **3** can differ accordingly (Figure S8 and S9). One of the major products of

SAT-KS-MAT + PT-ACP-TE reactions, in addition to **2** and **3**, was a set of coeluting octaketides **8** and **9**. Further fractionation revealed two isomeric C<sub>20</sub> products with masses corresponding to full-length species accompanied by loss of one water through cyclization and aromatization (Figure S11). These same products were also heavily represented in the SAT-KS-MAT + ACP and + ACP-TE reactions, leading to the hypothesis that they were spontaneously cyclized octaketide pyrones. For characterization, generation of these metabolites was optimized with respect to protein concentration. Increasing the ratio of ACP to SAT-KS-MAT above a minimum concentration threshold improved yields, as did inclusion of substoichiometric levels of the TE domain, consistent with its proposed editing function (Table S5). For large scale reactions, substrates were provided as SNAC thioesters. Hexanoyl-SNAC starter unit was synthesized from the acid chloride.<sup>19</sup> Malonyl-SNAC was generated *in situ* by the ATP-dependent ligation of malonate with SNAC by MatB, the malonyl coenzyme A synthetase from *Rhizobium leguminosarum*.<sup>16</sup> The diode array spectra, MS, and NMR analyses of the two distinct products were consistent with hexanoyl-primed analogs of SEK4 and SEK4b, commonly observed shunt metabolites of “minimal” type II<sup>27,28</sup> and engineered type III<sup>29,30</sup> octaketide synthases. Data in support of these structural assignments are provided in the Supporting Information (Figures S12–S17).

In addition to the pyrone derailment products discussed above, low levels of hydrolytically released products of shorter chain lengths were also observed (Figure 5). MS analysis of these species indicated that **13**, **14**, **15**, and **16** are truncated by one extension unit. Amounts of these species were diminished in reactions containing the TE domain and are likely released by spontaneous rather than enzyme-catalyzed hydrolysis. Heptaketides were not observed as enzyme-bound adducts on either the KS or ACP suggesting that their steady-state populations are below the detection limits of the acyl-enzyme MS assay. The presence of these species provides evidence of decreased processivity during the final extension cycle, perhaps owing to interruption by “sampling” in the PT domain.

Although noted previously for PksA,<sup>7</sup> it is worth reiterating that comparison of equivalent reactions that contain the same domain sets but different extents of interdomain links demonstrated that there is a penalty for catalysis *in trans*. In general, more intact enzyme combinations (with fewer components) led to improved fidelity and often efficiency compared to their more discrete counterparts. This is illustrated by juxtaposing reactions where PT and ACP were located on the same polypeptide as a didomain versus separately as two monodomains, where production of norpyrone (**4**) was 2-fold lower (Figure S9). Greater efficiency of intramolecular reactions through elevated effective concentration of intermediate substrates is thought to be a driving force behind the evolution of multidomain megasynthases from discrete proteins.<sup>31</sup> Sustained efforts to express PksA as an intact construct in *E. coli* for comparison have failed; however, one can expect fidelity and synthetic efficiency to improve in the native enzymatic environment where all domains are located on the same polypeptide.

**TE Editing.** To confirm that TE catalyzes release of aberrant adducts rather than just preventing their formation, its hydrolysis activity toward relevant acyl-enzyme and acyl-SNAC substrates was examined. In an initial experiment, <sup>14</sup>C-labeled acyl-ACP substrates were tested in the context of the ACP-TE didomain since these constructs were already in

hand.<sup>12</sup> ACP-TE was loaded with the Ppant arm from radiolabeled acetyl-, malonyl-, and hexanoyl-CoA catalyzed by Svp, a phosphopantetheinyl transferase (PPTase) from *Streptomyces venezuelae*.<sup>20</sup> Separation by SDS-PAGE and detection by autoradiography showed no retention of label for any substrate tested in reactions with an active TE (Figure S18A). In contrast, the TE mutant (S1937A) lacked hydrolysis activity and retained its radiochemical signal. Of note, in control reactions where Svp was excluded from the mixture, *holo*-ACP (present from partial *in vivo* activation during expression) self-acylated with acetyl and malonyl substrates, but not hexanoyl. ACP catalytic self-acylation has previously been demonstrated for the type II (discrete) PKS from actinorhodin biosynthesis<sup>32</sup> and may be a feature of the PksA ACP. Furthermore, TE had no detectable direct hydrolysis activity toward SAT, KS, or MAT (Figure S18B), indicating that TE-catalyzed hydrolysis is mediated through an acyl-ACP intermediate.

Since enzyme-bound MS data showed selective retention of malonyl-ACP in the TE-containing reactions, we considered that the lack of signal for malonyl in the didomain radiochemical assay could be a false positive and perhaps was due to spontaneous decarboxylation to acetyl prior to TE catalyzed hydrolysis during the extended incubation period. To address this concern, the ACP and TE were expressed independently so that domain concentrations and reaction time could be accurately controlled. Acyl-ACP hydrolysis activity was tested in a fixed time point assay with a 3-fold serial dilution of TE. The S1937A mutant was used as a negative control at only the highest concentration tested for wild-type enzyme. Assays showed that hexanoyl- and acetyl-ACP were actively hydrolyzed by TE and that malonyl-ACP was not detected as a substrate (Figure 6A). These results are in agreement with enzyme-bound MS data where the extent of hexanoyl and acetyl acylation was drastically reduced or eliminated in reaction combinations containing TE, whereas malonyl was minimally affected by its presence.

To follow up the acyl-ACP results, kinetic parameters were determined for TE catalyzed acetyl- and hexanoyl-SNAC hydrolysis by an established continuous spectrophotometric assay employing Ellman's reagent for detection of released SNAC.<sup>17</sup> The kinetic parameters are summarized in Figure 6B and Michaelis–Menten plots showing hydrolysis rate as a function of substrate concentration are given in Figure S19. The inactive TE mutant was used as a negative control for background correction. The 12-fold difference in catalytic efficiency ( $k_{\text{cat}}/K_{\text{M}}$ ) for hydrolysis of hexanoyl ( $32.3 \text{ M}^{-1}\text{sec}^{-1}$ ) over acetyl ( $2.6 \text{ M}^{-1}\text{sec}^{-1}$ ) is almost exclusively due to reduced binding affinity. Although kinetic parameters for the acyl-ACP substrates were not determined, ACP-bound hexanoyl is cleaved at a faster relative rate than acetyl, mirroring the reduced affinity observed for the analogous SNAC analogs. It is expected that domain–domain interactions between ACP and TE within the multidomain synthase would accelerate hydrolysis rates.

Next, we examined the editing role of TE in a reaction setting. PT was excluded to prevent production of intermediate **7** and effectively decouple Claisen cyclization from TE's editing activity, instigating spontaneous derailment at the linear polyketide stage. The peak areas of major reaction products—hex-SEK4 (**8**), hex-SEK4b (**9**), and triketide pyrone **11**—were monitored as a function of TE concentration. SAT-KS-MAT and ACP were held constant at  $10 \mu\text{M}$  and TE was varied from 0 to  $40 \mu\text{M}$  using acyl-CoAs as substrates. Plotting



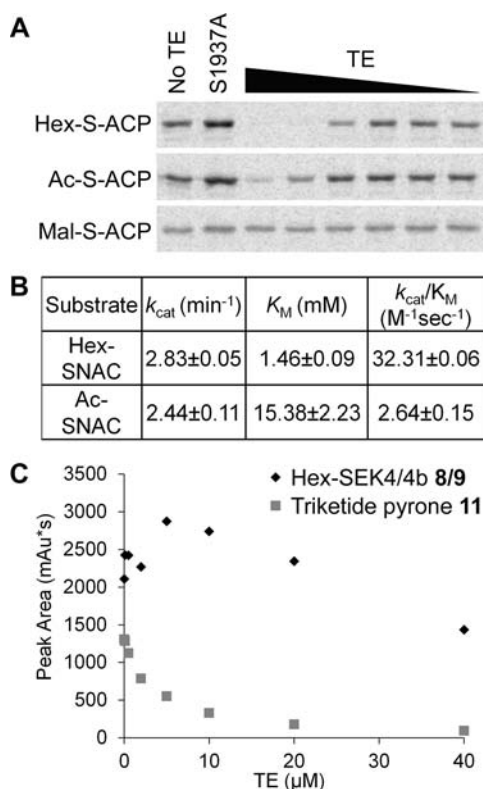


**Figure 6.** Editing function of PksA TE. (A) <sup>14</sup>C-acyl-ACP hydrolysis assay toward hexanoyl, acetyl, and malonyl species. Acyl-ACP (10 μM) was treated with no TE, TE-S1937A (3 μM), or TE (3, 1, 0.33, 0.11, 0.04, or 0.01 μM) for 6 min. Proteins were separated by SDS-PAGE and phosphorimaged. (B) Kinetic constants for TE catalyzed acyl-SNAC hydrolysis from a continuous UV-vis spectrophotometric assay using Ellman's reagent. (C) PksA product titers are dependent on TE concentration. Constant SAT-KS-MAT and ACP (10 μM each) were combined with variable TE (0, 0.1, 0.5, 2, 5, 10, 20, or 40 μM).

the yield of 8/9 (as coelvents) against TE concentration demonstrated that production of the full-length spontaneous cyclization products was maximized at 5 μM (half stoichiometry relative to the other domains) and dropped off steadily to approximately 50% of peak production at 40 μM (Figure 6C). In contrast, production of 11 gradually decreased over the entire range. Although the overall yield of polyketide metabolites diminished with increasing levels of TE, fidelity in producing only full-length products improved.

**Attempts to Observe Intermediate Chain-length Polyketides.** In an effort to visualize partially extended intermediates on PksA, a nonhydrolyzable malonyl CoA analog 17, first developed by Tosin et al. to trap polyketides from a type III PKS system as CoA adducts, was synthesized.<sup>22</sup> Type III PKSs, like the stilbene synthase used in this Tosin/Leadlay study, lack carrier proteins and instead use CoA thioesters directly to sustain the growing polyketide. The dethia malonyl-CoA analog 17, where the labile thioester sulfur is replaced by a methylene, was synthesized by established methods.<sup>22</sup> This species can still undergo decarboxylative Claisen condensation, but can no longer transfer back to the KS for further extension. To adapt the analog to our system, apo-ACP was "activated" with the analog using the Svp PPTase (Figure 7). Despite attempts to optimize reaction conditions to trap polyketide intermediates on the ACP by varying protein ratios and substrate concentrations, only the decarboxylated analog and

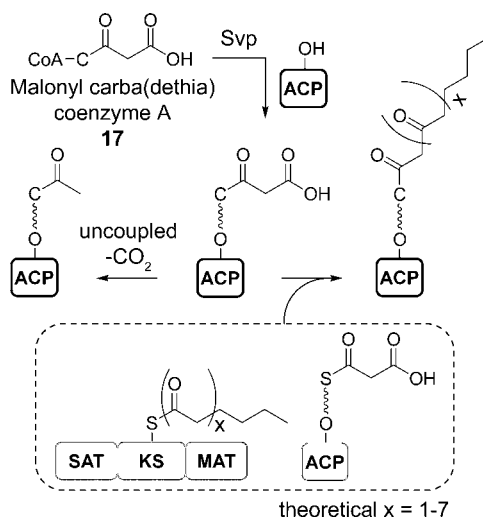


**Figure 7.** Polyketide assembly by PksA was not interrupted by a nonhydrolyzable malonyl analog. Apo-ACP was activated with the analog 17, and reacted with SAT-KS-MAT and *holo*-ACP. Only the starter unit condensed with the analog ( $x = 1$ ), and the uncoupled decarboxylation products were detected.

the diketide (one extension) products were observed, providing further evidence of high polyketide extension processivity. Once initiated, condensation to the full-length octaketide occurred without interruption by the analog. Pentanoyl and heptanoyl were also provided in the form of acyl-SNAC thioesters with the hope that the noncognate starter units would retard transacylation of the growing polyketide chain and allow interception of truncated polyketides; however, results were similar to hexanoyl primed reactions, producing only the one extension ACP-bound products (Figure S22 and Table S9).

Assuming that processivity would be dependent on the rapid reacylation of the ACP with malonyl following chain transfer to the KS, we hypothesized that a decrease in rate of MAT transacylase activity could be a potential route to enable off-loading of KS-bound intermediate chain-length polyketides by the nonhydrolyzable analog. Smith and co-workers reported a reduction in rate for malonyl transfer by the MAT domain of animal FAS when an arginine residue important for substrate binding was mutated.<sup>25</sup> MAT mutants R606K and R606A caused a 100- and 1000-fold decrease in transacylase activity, respectively. These results were attributed to loss of a salt bridge between the carboxylate of malonyl and the guanidinium of Arg606. Sequence alignments demonstrated that this arginine was conserved among NR-PKS MAT domains (Figure S23A). The analogous position in PksA MAT (Arg1018) was mutated to Lys, however, expression attempts of this SAT-KS-MAT mutant construct in *E. coli* failed to yield enough soluble protein for analysis. Surprisingly, the less conservative Ala mutant was readily overproduced, but when utilized in *in vitro* reactions, it proved incapable of accumulating polyketide products. Attempted chemical complementation of the R1018A mutant with guanidinium ion (at 0.1, 0.5, or 1 M concentrations) failed to restore production (Table S23B).

**Transacylase Activity.** The relative rates of hexanoyl and malonyl transfer were determined by an established HPLC-based chromatographic transacylase assay using acyl-CoA donor and pantetheine acceptor molecules.<sup>9</sup> Transferase activity of the PksA SAT monodomain was previously

determined using this method.<sup>24</sup> In this study, we expanded the subjects to multidomain fragments to see if the presence of additional domains would affect transfer rates and to facilitate analysis of KS and MAT activities. In our experience, KS monodomains are particularly resistant to heterologous expression. Production of the PksA MAT has only been achieved through extensive trouble shooting of cut sites and refolding the enzyme from inclusion bodies.<sup>33</sup> The activity of KS and MAT were therefore measured in the context of the readily expressed SAT-KS-MAT tridomain in which the individual activity of each domain was isolated by inactivating mutation of the other two.

SAT hexanoyl transferase activity was enhanced approximately 3-fold in the context of the tridomain relative to the monodomain, providing evidence that interdomain associations improve catalytic efficiency (Figure 8A). Malonyl transfer by

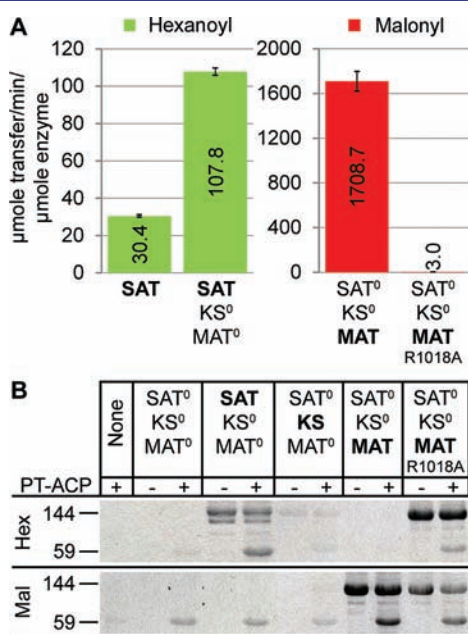


**Figure 8.** Transacylase activities of PksA domains. (A) RPLC-based transacylase assay. SAT monodomain hexanoyl transfer rate was previously determined.<sup>24</sup> (B) <sup>14</sup>C-acyl-CoA transacylase assay. SAT-KS-MAT (144 kDa) and PT-ACP (59 kDa) were treated with hexanoyl (top panel) or malonyl (lower panel). The symbol <sup>0</sup> denotes a loss-of-function mutant which has the active site nucleophile removed by mutation to an alanine.

MAT was measured at 16 times the rate of hexanoyl transfer by SAT in the tridomain, supporting, at least in part, a kinetic basis for processivity of polyketide extension. Malonyl transfer was greatly retarded by the R1018A mutation, showing a 560-fold drop in transacylase rate relative to wild-type (Figure 8B). This difference is comparable to the 1000-fold decrease in catalytic efficiency observed for the analogous mutation in rat FAS.<sup>25</sup>

Although this assay gives a measurement of relative rates of acyl transfer, it does not take into account the role of protein–protein interactions between donor and acceptor domains since pantetheine is used as a surrogate acceptor *in lieu* of *holo*-ACP. Therefore, the ability of SAT-KS-MAT mutants to load <sup>14</sup>C-labeled hexanoyl and malonyl groups from CoA substrates onto the PT-ACP didomain was examined. TE was excluded due to its hydrolytic editing activity. Proteins were separated by SDS-PAGE and imaged by autoradiography (Figure 8B). The results

were consistent with the proposed activity of each domain and with data collected from active site occupancy studies and pantetheine acceptor transacylase assays. SAT loads and transfers hexanoyl only. To a limited extent KS is able to directly acylate with hexanoyl-CoA providing an alternative route for polyketide chain initiation. This observation could explain why some enzymes with nonfunctional SAT domains are still able to biosynthesize polyketides *in vitro* where superphysiological substrate concentrations can be maintained.<sup>13</sup> Interestingly, mutation of Arg1018 altered the substrate specificity of the MAT domain. In addition to transferring malonyl, albeit at a slower rate than the wild-type enzyme, MAT R1018A could additionally transfer hexanoyl onto ACP. A similar change in substrate selectivity has been observed for another MAT domain. The analogous R606A mutant from rat FAS exhibited greater than three orders-of-magnitude increase in transacylase activity toward octanoyl relative to the wild-type enzyme.<sup>25</sup> Structural characterization of human MAT and substrate docking with various acyl-CoAs demonstrated that mutation of arginine to the smaller alanine residue gives access to a cryptic binding pocket at the interface of two subdomains.<sup>34</sup> Increased acylation of this MAT mutant with hexanoyl explains why recombination experiments with it failed to turn over. As observed in the TE hydrolysis assay control experiment, ACP self-acylated with malonyl but not hexanoyl.

## DISCUSSION

Three main features of PksA catalysis contributing to biosynthetic fidelity highlighted by this study are processivity in polyketide extension, “balanced domain occupancy”, and editing of aberrant species by the C-terminal TE domain. These features are particularly important for iterative classes of enzymes that rely on repeated use of catalytic domains since any nonproductive decarboxylation, cyclization, or substrate priming could stall biosynthesis for the entire complex. Through profiling the occupancy of multiple active sites and biosynthetic output in parallel, combined with functional assays to target individual domain activities, a far deeper understanding of iterative polyketide catalysis for NR-PKs has been established.

Although modular and iterative PKs both catalyze decarboxylative thio-Claisen condensations with malonyl extension units, the requirements on substrate specificity for their KS active sites differ greatly. Domains involved in iterative catalysis must bind all lengths of polyketide intermediates that exist en route from the acyl starter unit to the programmed full-length oligoketide. In many ways, the range of substrate specificities and orchestration of repeated domain use are more akin to iterative assembly of fatty acids. NR-PKs are believed to be structurally related to the mammalian FASs where the KS and DH-like PT domains make up the core of the dimeric megasynthase complex.<sup>11</sup> In FAS, successive chain extensions are interrupted by catalysis in the KR, DH, and ER domains. Whereas the alkyl chain of the growing fatty acid is inert to further chemical reaction, NR-PKs have the special requirement of stabilizing highly reactive, linear poly- $\beta$ -ketides. Since no “tailoring” occurs at the  $\beta$ -carbon, there is no requisite for the elongating chain to leave the KS active site. Condensation with malonyl-ACP and immediate transesterification back to the KS could occur by simply shifting the extended polyketide deeper into the KS binding pocket hence protecting it from spurious cyclization.

The absence of observable extended adducts on the KS, the high occupancy of the MAT domain, the fast rate of malonyl transfer, and the inability of a nonhydrolyzable malonyl analog to interrupt assembling polyketides all point to a general model where extension of the starter unit is rapid and processive. Two subunits each of HexA, HexB, and PksA comprise the norsolorinic acid anthrone synthase (NorS) as determined by size-exclusion chromatography of the wild-type complex isolated from the native *Aspergillus*.<sup>35</sup> The associated FAS (HexA/B) is proposed to directly transacylate the hexanoyl starter unit onto the SAT domain.<sup>36</sup> The conformational changes that must occur to enable SAT to dock with both the HexA ACP and PksA ACP may be a slow step in the overall catalysis. Rapid extension of hexanoyl, once loaded, would account for its observed low abundance on the enzyme.

Another strategy for maintaining biosynthetic fidelity appears to be coordinated domain use based on substrate specificity and negative cooperativity. Such constraints on domain activities would naturally lead to the observed “balanced domain occupancy” of PksA by preventing overcongestion with any one particular substrate or intermediate and allowing extension pathways to prevail. MAT acylation seems to be independent of other domains, whereas SAT and KS activities appear to be linked. Indirect evidence for cooperativity of SAT and KS function is provided by several observations. First, both SAT and KS have low levels of substrate bound (Figure 3). This is consistent with studies on yeast and animal multidomain primary metabolic FASs where substoichiometric loading of acetyl and malonyl was observed for <sup>14</sup>C-labeled substrates.<sup>37</sup> Partial occupancy of FAS active sites was argued as evidence for negative cooperativity of domain functions. Second, production of the hexanoyl primed tetraketide and triketide pyrones, **10** and **11**, from SAT-KS-MAT-only reactions was improved by inactivating the SAT domain (Figure S10). Blocking SAT acylation resulted in an apparent increase in KS activity, which indicates that KS-catalyzed condensation is likely suppressed by starter unit-binding in the neighboring SAT domain. Third, over a 3-fold increase in relative hexanoyl transacylase activity of SAT in the tridomain versus the monodomain was observed (Figure 8A). Conformational changes triggered by intermediate binding likely translate to other domains through quaternary, allosteric interactions.

ACP is the hub of thiotemplated biosynthesis, interacting with all other domains. Protein–protein interactions between ACP and its client domains have been shown in other systems to be dependent on the bound acyl species<sup>38,39</sup> and this is likely the case for PksA as well. In PksA the extent of overall ACP occupancy was diminished for bisubstrate reactions compared to malonyl-only incubations (Figure 4), indicating that the presence of hexanoyl and extending polyketides prevents ACP saturation with malonyl. Maintaining balanced domain occupancy ensures that acyl binding sites are available for polyketide elongation and that substrates are provided on a just-in-time basis.

In contrast to NR-PKSs, active site occupancy analyses of modular PKSs suggest that crowding with intermediates ensures synthetic fidelity. One of the most highly studied systems is the yersiniabactin NRPS/PKS hybrid consisting of two high molecular weight proteins. A “crawling model”, where active sites are highly occupied and all intermediates are moved forward with rapid reacylation of the condensation domains to prevent back transfer of the growing intermediate has been proposed.<sup>40</sup> Investigations of the erythromycin modular type I

PKS megasynthase (DEBS) have brought forth a similar “congestion model” where chain extension cycles are triggered by TE release from the last module.<sup>41</sup>

MS interrogation of active site peptides of iterative synthases has been limited. In our laboratory, we previously looked at the PksA ACP occupancy,<sup>7</sup> which was expanded upon in this study to four additional domains. Recently, the diketide synthase (LovF) responsible for generation of the  $\alpha$ -butyrate side chain in lovastatin biosynthesis in *Aspergillus terreus* was examined.<sup>42</sup> Although its domain architecture resembles iterative highly reducing (HR-) PKS, it is not an iterative enzyme. Rather an acetyl starter unit is condensed with a single malonyl extension unit, which undergoes stereospecific methylation and full reduction at the  $\beta$ -carbon. The diketide product of LovF is appended onto monocolin J by the LovD acyltransferase to synthesize lovastatin. Analysis of Ppant ejection ions resulted in detection of five predicted ACP-bound intermediates. In contrast to PksA, which exhibited low ACP acylation when all substrates were provided, the LovF ACP was highly occupied. Due to the limited number of examples, it is impossible to discern if the extent of ACP acylation is a general differentiating feature between HR-PKS and NR-PKS or a result of the specific reaction conditions tested.

An additional device employed by PksA to preserve faithful biosynthesis is basal editing carried out by the C-terminal TE domain. Since catalysis is iterative, any deviation from on-target pathways risks derailing the enzyme into nonproductive states. Spontaneous hydrolysis is a slow process and the evolutionary advantage to maintaining net synthetic function in a background of enzyme-mediated hydrolysis of aberrant species is apparent. Two types of TEs are recognized in natural product pathways, biosynthetic and editing. Regardless of their function, TEs generally belong to the  $\alpha/\beta$  hydrolase family and contain a conserved Ser-His-Asp catalytic triad and “oxyanion hole” for stabilization of the tetrahedral transition state. Biosynthetic TEs are responsible for product release—catalyzing hydrolysis, macrocyclization, or Claisen/Dieckmann cyclization to release the final covalent intermediate.<sup>43</sup> Disruption of biosynthetic TEs decimates production of the natural product. Discrete, type II editing TEs are associated with bacterial modular PKS and NRPS biosynthetic pathways. Examples include the pikromycin and rifamycin TEIs from a modular type I PKS and hybrid PKS-NRPS, respectively.<sup>44,45</sup> Genomic deletion of type II editing TEs typically results in decreased titers of the natural product, an outcome ascribed to the accumulation of nonproductive intermediates on the enzyme, thus blocking biosynthesis. Consistent with this editing function, overproduction of TEIs can also negatively affect biosynthetic output by competing for productive pathways.

To our knowledge no editing-type TEs have been implicated in fungal iterative PKS catalysis. *In vitro* experiments with the dissected PksA TE mirror results for both biosynthetic- and editing-type TEs. Enzymatic synthesis of noranthrone (**2**) is dependent on inclusion of the TE domain to catalyze Claisen cyclization for its release (Figure 5). In PT-less reactions where TE concentration was varied, titers of hex-SEK4 (**8**) and hex-SEK4b (**9**) were highest when TE was provided at half-stoichiometry relative to the SAT-KS-MAT and ACP domains (Figure 6C). Furthermore, synthesis of the triketide derailment product **11** steadily declined with increasing concentrations of TE, indicating that improved biosynthetic fidelity to the linear octaketide **5** came at the cost of overall production.



The recently published 1.7 Å crystal structure of the dissected C-terminal PksA TE domain shows an internal hydrophobic reaction chamber containing the catalytic triad that is isolated from its aqueous environment by a flexible lid motif.<sup>12</sup> Lid opening is proposed to facilitate delivery of ACP-bound Ppant thioester substrates. Structures of stand-alone editing TEs have been determined and show increased flexibility in the lid region compared to their biosynthetic type I counterparts (e.g., Srf TEI<sup>46</sup> and TEII<sup>47</sup>). The active site pocket of PksA is sufficiently malleable to accept alternative substrates to the native bicyclic intermediate 7, and was able to hydrolyze acetyl, hexanoyl, and benzoyl,<sup>6</sup> but not malonyl. A “low specificity model” has been proposed for bacterial TEIs where slow kinetics of thioester hydrolysis, rather than tight substrate specificity, guides editing.<sup>45</sup> Since correct substrates and extending intermediates are favored for productive pathways, aberrant species are preferentially hydrolyzed due to their presumably long relative lifetimes on the carrier domain. We believe that PksA TE is a similar case, hydrolyzing both on-pathway species (e.g., hexanoyl) and nonproductive species (e.g., acetyl) from the ACP. The fate of the hexanoyl starter unit is partitioned between competing pathways for transfer from ACP to the KS for polyketide extension or to the TE for hydrolysis. This phenomenon could have ramifications for engineering of novel polyketides through incorporation of unnatural starter units. Reduced specificity of the KS domain toward alternative substrates may slow the kinetics of oligoketide assembly enough to allow TE hydrolysis to more readily compete, thus reducing or preventing accumulation of extended products in reactions possessing an active TE.

Taking into account all of the above information, we summarize here the “checks and balances” overseeing polyketide assembly by NR-PKSs. The N-terminal SAT domain is the first gatekeeper. In PksA, a hexanoyl starter is provided (likely directly) by a dedicated FAS and is transferred to the ACP by the SAT domain to initiate synthesis. Such an arrangement is, however, a special case. Typically, acetyl-CoA is the preferred substrate of most SATs and selecting appropriate starter units from the pool of available acyl-CoAs is the initial checkpoint for orchestrating biosynthetic fidelity. Loading of the KS with starter unit triggers the synthase to begin iterative condensation cycles with malonyl extender units. KS decarboxylase activity appears to be restricted to when appropriate intermediates are present and acetyl-ACP does not accumulate when no starter unit is in place. The KS active site is maintained in a net vacant state ensuring that intermediates do not become stalled there. Aided by high malonyl occupancy of the MAT domain, extension is rapid and successfully outcompetes spurious cyclization of the tethered transitional chain-length species. The complex balance of KS functions that emerges from these data comprises the second checkpoint of NR-PKS programming. Passive protection of the poly- $\beta$ -keto intermediates may additionally be conferred through sequestration of the growing chain in the KS binding pocket or possibly the PT domain, especially as the final chain length is approached. Structural characterization of the dissected PksA ACP in *holo*- and hexanoyl-forms demonstrated that starter unit is not sequestered in this fungal type I domain.<sup>48</sup> Extrapolating from this lack of binding, the ACP domain may not actively be involved in intermediate stabilization, as has been observed for bacterial type II ACPs.<sup>49</sup> Detection of low levels of truncated products in reaction extracts suggests that as the oligoketide nears its

programmed chain length, it may leave the KS active site, owing to decreased processivity during the final extensions, and be subject to spontaneous cyclization and hydrolysis. Full-length octaketide species prevailed under all experimental conditions tested (except in the absence of the ACP domain) and chain length is principally controlled by the KS. Regiospecific cyclizations and dehydrations of the linear  $\beta$ -keto intermediate by PT are comparatively slow steps in overall NR-PKS catalysis and constitute the final important checkpoints of biosynthesis. The accumulation of incrementally cyclized species (5–7) on the ACP suggests that the linear polyketide and the two cyclic intermediates are reversibly bound in the PT domain in the time regime of synthesis to be individually detectable by mass spectrometry.<sup>7</sup> Transesterification of the PT-cyclized product to the TE domain may similarly be a slow step. TE/CLC has two functions: editing as a housekeeping measure to remove stalled intermediates and catalyzing terminal Claisen/Dieckmann cyclization of mature polyketides for product release. Some NR-PKSs will be more “perfect” than others in faithfully producing their intended aromatic product, but the ways in which catalytic efficiency is achieved (kinetic and allosteric interdomain effects combined with background editing functions to maximize the net flux of synthesis) will likely be conserved.

## CONCLUSION

Thiotemplated biosynthesis of polyketides, nonribosomal peptides, and fatty acids relies on the timely delivery of appropriate substrates and intermediates to correct active sites. Because substrates and intermediates are covalently bound to the enzyme during biosynthesis, few tools are available to view intermediate stages of their assembly. The advancement of MS methods to interrogate acylation profiles of active site peptides has revolutionized the analysis of natural product biosynthesis. In our present investigation, the complete set of active site peptides from all five domains of PksA that form covalent reaction adducts were identified and simultaneously monitored to provide a global portrait of covalent occupancy. The only other system interrogated at a comparable level is that of yersiniabactin.<sup>40</sup> The acylation profiles and subsequent *in vitro* biochemical analyses indicate an evolved balance of kinetic and cooperative controls facilitate correct order of substrate priming, elongation, and cyclization events. High sequence similarity and common domain architectures for members of the NR-PKS family of enzymes argues that the rules governing iterative catalysis by PksA will translate to other enzymes of this type.

## ASSOCIATED CONTENT

### Supporting Information

Additional experimental methods and results. This material is available free of charge via the Internet at <http://pubs.acs.org>.

## AUTHOR INFORMATION

### Corresponding Author

\*ctownsend@jhu.edu

### Notes

The authors declare no competing financial interest.

## ACKNOWLEDGMENTS

We thank Drs. M. Adams and J. R. Scheerer and E. A. Hill for synthesis of acyl-SNAC substrates. We are grateful to Dr. K. A.

Moshos for advice on the synthesis of the nonhydrolyzable malonate analog and Dr. R. F. Li for cloning the *matB* gene. CoA biosynthetic enzyme expression plasmids were a kind gift of Prof. G. D. Wright (McMaster University, Hamilton, Ontario). We also thank Dr. A. Majumdar and the facilities and resources provided by the Johns Hopkins University Biomolecular NMR Center, J. M. McCaffery and the Johns Hopkins University Integrated Imaging Center for use of their phosphorimager, and K. L. Fiedler and Prof. R. J. Cotter of the Middle Atlantic Mass Spectrometry Laboratory at the Johns Hopkins School of Medicine and the Mid-Atlantic Regional Office of Shimadzu Scientific Instruments, Inc. (Columbia, MD) for use of their Shimadzu LC-IT-TOF. Financial Support was provided by the National Institute of Health grant numbers GM 067725 and NIH ES001670.

## REFERENCES

- (1) Dorrestein, P. C.; Kelleher, N. L. *Nat. Prod. Rep.* **2006**, *23*, 893–918.
- (2) Evans, B. S.; Robinson, S. J.; Kelleher, N. L. *Fungal Genet. Biol.* **2011**, *48*, 49–61.
- (3) Dorrestein, P. C.; Bumpus, S. B.; Calderone, C. T.; Garneau-Tsodikova, S.; Aron, Z. D.; Straight, P. D.; Kolter, R.; Walsh, C. T.; Kelleher, N. L. *Biochemistry* **2006**, *45*, 12756–12766.
- (4) Jenke-Kodama, H.; Dittmann, E. *Phytochemistry* **2009**, *70*, 1858–1866.
- (5) Cox, R. J.; Simpson, T. J. *Methods in Enzymology*; David, A. H., Ed.; Academic Press: New York, 2009; Vol. 459, pp 49–78.
- (6) Udworthy, D. W.; Merski, M.; Townsend, C. A. *J. Mol. Biol.* **2002**, *323*, 585–598.
- (7) Crawford, J. M.; Thomas, P. M.; Scheerer, J. R.; Vagstad, A. L.; Kelleher, N. L.; Townsend, C. A. *Science* **2008**, *320*, 243–246.
- (8) Crawford, J. M.; Townsend, C. A. *Nat. Rev. Microbiol.* **2010**, *8*, 879–889.
- (9) Crawford, J. M.; Dancy, B. C. R.; Hill, E. A.; Udworthy, D. W.; Townsend, C. A. *Proc. Natl. Acad. Sci. U.S.A.* **2006**, *103*, 16728–16733.
- (10) Ehrlich, K. C.; Li, P.; Scharfenstein, L.; Chang, P.-K. *Appl. Environ. Microbiol.* **2010**, *76*, 3374–3377.
- (11) Crawford, J. M.; Korman, T. P.; Labonte, J. W.; Vagstad, A. L.; Hill, E. A.; Kamari-Bidkorpeh, O.; Tsai, S.-C.; Townsend, C. A. *Nature* **2009**, *461*, 1139–1143.
- (12) Korman, T. P.; Crawford, J. M.; Labonte, J. W.; Newman, A. G.; Wong, J.; Townsend, C. A.; Tsai, S.-C. *Proc. Natl. Acad. Sci. U.S.A.* **2010**, *107*, 6246–6251.
- (13) Ma, S. M.; Zhan, J.; Watanabe, K.; Xie, X.; Zhang, W.; Wang, C. C.; Tang, Y. *J. Am. Chem. Soc.* **2007**, *129*, 10642–10643.
- (14) Szewczyk, E.; Chiang, Y.-M.; Oakley, C. E.; Davidson, A. D.; Wang, C. C. C.; Oakley, B. R. *Appl. Environ. Microbiol.* **2008**, *74*, 7607–7612.
- (15) Sambrook, J.; Russell, D. W. *Molecular Cloning: A Laboratory Manual*; Cold Spring Harbor Laboratory Press: Cold Spring Harbor, NY, 2001.
- (16) An, J. H.; Kim, Y. S. *Eur. J. Biochem.* **1998**, *257*, 395–402.
- (17) Heathcote, M. L.; Staunton, J.; Leadlay, P. F. *Chem. Biol.* **2001**, *8*, 207–220.
- (18) Riddles, P. W.; Blakeley, R. L.; Zerner, B.; C.H.W. Hirs, S. N. T. In *Methods in Enzymology*; Academic Press: New York, 1983; Vol. 91, pp 49–60.
- (19) Brobst, S. W.; Townsend, C. A. *Can. J. Chem.* **1994**, *72*, 200–207.
- (20) Sanchez, C.; Du, L.; Edwards, D. J.; Toney, M. D.; Shen, B. *Chem. Biol.* **2001**, *8*, 725–738.
- (21) Beltran-Alvarez, P.; Cox, R. J.; Crosby, J.; Simpson, T. J. *Biochemistry* **2007**, *46*, 14672–14681.
- (22) Tosin, M.; Dieter, S.; Jonathan, B. S. *ChemBioChem* **2009**, *10*, 1714–1723.
- (23) Nazi, I.; Koteva, K. P.; Wright, G. D. *Anal. Biochem.* **2004**, *324*, 100–105.
- (24) Crawford, J. M.; Vagstad, A. L.; Whitworth, K. P.; Ehrlich, K. C.; Townsend, C. A. *ChemBioChem* **2008**, *9*, 1019–1023.
- (25) Rangan, V. S.; Smith, S. J. *Biol. Chem.* **1997**, *272*, 11975–11978.
- (26) Yalpani, M.; Willecke, K.; Lynen, F. *Eur. J. Biochem.* **1969**, *8*, 495–502.
- (27) Fu, H.; Ebert-Khosla, S.; Hopwood, D. A.; Khosla, C. *J. Am. Chem. Soc.* **1994**, *116*, 4166–4170.
- (28) Fu, H.; Hopwood, D.; Khosla, C. *Chem. Biol.* **1994**, *1*, 205–210.
- (29) Abe, I.; Watanabe, T.; Morita, H.; Kohno, T.; Noguchi, H. *Org. Lett.* **2006**, *8*, 499–502.
- (30) Karppinen, K.; Hokkanen, J.; Mattila, S.; Neubauer, P.; Hohtola, A. *FEBS J.* **2008**, *275*, 4329–4342.
- (31) Vogel, C.; Bashton, M.; Kerrison, N. D.; Chothia, C.; Teichmann, S. A. *Curr. Opin. Struct. Biol.* **2004**, *14*, 208–216.
- (32) Hitchman, T. S.; Crosby, J.; Byrom, K. J.; Cox, R. J.; Simpson, T. J. *Chem. Biol.* **1998**, *5*, 35–47.
- (33) Ma, Y.; Smith, L. H.; Cox, R. J.; Beltran-Alvarez, P.; Arthur, C. J.; FRS, T. J. S. *ChemBioChem* **2006**, *7*, 1951–1958.
- (34) Bunkoczi, G.; Misquitta, S.; Wu, X.; Lee, W. H.; Rojkova, A.; Kochan, G.; Kavanagh, K. L.; Oppermann, U.; Smith, S. *Chem. Biol.* **2009**, *16*, 667–675.
- (35) Watanabe, C. M. H.; Townsend, C. A. *Chem. Biol.* **2002**, *9*, 981–988.
- (36) Watanabe, C. M. H.; Wilson, D.; Linz, J. E.; Townsend, C. A. *Chem. Biol.* **1996**, *3*, 463–469.
- (37) Schweizer, E.; Hofmann, J. *Microbiol. Mol. Biol. Rev.* **2004**, *68*, 501–517.
- (38) Tran, L.; Tosin, M.; Spencer, J. B.; Leadlay, P. F.; Weissman, K. J. *ChemBioChem* **2008**, *9*, 905–915.
- (39) Płoskoń, E.; Arthur, C. J.; Kanari, A. L. P.; Wattana-amorn, P.; Williams, C.; Crosby, J.; Simpson, T. J.; Willis, C. L.; Crump, M. P. *Chem. Biol.* **2010**, *17*, 776–785.
- (40) McLoughlin, S. M.; Kelleher, N. L. *J. Am. Chem. Soc.* **2004**, *126*, 13265–13275.
- (41) Hong, H.; Leadlay, P. F.; Staunton, J. *FEBS J.* **2009**, *276*, 7057–7069.
- (42) Meehan, M. J.; Xie, X.; Zhao, X.; Xu, W.; Tang, Y.; Dorrestein, P. C. *Biochemistry* **2010**, *50*, 287–299.
- (43) Du, L.; Lou, L. *Nat. Prod. Rep.* **2010**, *27*, 255–278.
- (44) Kim, B. S.; Cropp, T. A.; Beck, B. J.; Sherman, D. H.; Reynolds, K. A. *J. Biol. Chem.* **2002**, *277*, 48028–48034.
- (45) Claxton, H. B.; Akey, D. L.; Silver, M. K.; Admiraal, S. J.; Smith, J. L. *J. Biol. Chem.* **2009**, *284*, 5021–5029.
- (46) Bruner, S. D.; Weber, T.; Kohli, R. M.; Schwarzer, D.; Marahiel, M. A.; Walsh, C. T.; Stubbs, M. T. *Structure* **2002**, *10*, 301–310.
- (47) Koglin, A.; Lohr, F.; Bernhard, F.; Rogov, V. V.; Frueh, D. P.; Strieter, E. R.; Mofid, M. R.; Guntert, P.; Wagner, G.; Walsh, C. T.; Marahiel, M. A.; Dotsch, V. *Nature* **2008**, *454*, 907–911.
- (48) Wattana-amorn, P.; Williams, C.; Płoskoń, E.; Cox, R. J.; Simpson, T. J.; Crosby, J.; Crump, M. P. *Biochemistry* **2010**, *49*, 2186–2193.
- (49) Evans, S. E.; Williams, C.; Arthur, C. J.; Płoskoń, E.; Wattana-amorn, P.; Cox, R. J.; Crosby, J.; Willis, C. L.; Simpson, T. J.; Crump, M. P. *J. Mol. Biol.* **2009**, *389*, 511–528.